Stream gains and losses across a mountain-to-valley transition: Impacts on watershed hydrology and stream water chemistry

Timothy P. Covino[1] and Brian L. McGlynn[1]

Received 3 October 2006; revised 22 May 2007; accepted 16 July 2007; published 26 October 2007.

[1] The mountain to alluvial valley transition is a dominant landscape of the American West, and of mountainous regions around the world, and is crucial to water resources in these regions. We combined stream water and groundwater (GW) hydrometric methods with geochemical hydrograph separations to investigate stream gains and losses across a mountain to alluvial valley transition in southwestern Montana to address the following questions: (1) How do alpine to valley bottom transitions affect stream discharge? (2) How do stream gains and losses change across alpine to valley bottom transitions? There was an annual 23% net loss in stream discharge across the transition zone, which we refer to as the mountain front recharge (MFR) zone. Gross stream gains were minimal in the MFR zone. Gross stream losses across the valley bottom equaled $\sim$140,000 m^3 while gross gains equaled $\sim$70,000 m^3, resulting in a net loss of $\sim$70,000 m^3 in the valley bottom zone. Stream discharge was 97% alpine runoff (AL) in the MFR zone, whereas downstream discharge in the valley bottom was 48% AL and 52% valley groundwater. These large spatial and long temporal scale exchanges of water across the mountain-to-valley transition affected stream discharge magnitude, valley aquifer storage state, and valley stream water chemistry. This work suggests that streams do not simply lose or gain over a particular reach, but rather many streams are both gaining and losing and that net differences yield an incomplete depiction of stream hydrology.

Citation: Covino, T. P., and B. L. McGlynn (2007), Stream gains and losses across a mountain-to-valley transition: Impacts on watershed hydrology and stream water chemistry, *Water Resour. Res.*, *43*, W10431, doi:10.1029/2006WR005544.

1. Introduction

[2] The realization that streams and surrounding groundwater (GW) exist as a connected resource has helped to advance the fields of hydrology, biogeochemistry, and aquatic ecology. Stream losses to GW and gains from GW play an important role in the processes that affect watershed hydrologic response, water quality, and subsequent impacts on aquatic biota. The exchange of water between streams and GW has been noted as an important mechanism for solute and contaminant transport [*Ren and Packman*, 2005]; dissolved organic carbon (DOC) cycling [*Wagner and Beisser*, 2005]; lotic ecosystem processes [*Wroblicky et al.*, 1998]; and water resource management [*Oxtobee and Novakowski*, 2002]. These exchanges occur at multiple scales across the landscape. *Harvey et al.* [1996] define smaller-scale exchanges as those that occur at centimeter-long flow paths and timescales of minutes, and larger-scale exchanges as those that occur over hundreds of meters and timescales of years. Many studies of stream water–GW exchanges have focused on small spatial- and temporal-scale interactions. In this paper we use exchange to refer to stream losses to and gains from GW. The focus of our research is to investigate how stream losses and gains (at the larger scale noted above) to and from local GW impact hydrologic response, source water contributions, and stream water chemistry across a mountain-to-valley transition.

[3] Hydrologists, biogeochemists, and ecologists have become interested in the stream water–GW exchanges that occur in the hyporheic zone (HZ), and considerable improvements in understanding have been made in this area. Advances in the study of the HZ have been crucial to developing the link between streams and GW, and the HZ is now viewed as an integral part of the stream itself [*Malard et al.*, 2002]. HZ interactions occur on small scales that exist embedded within a larger framework of stream water–GW exchanges. At the larger scale, stream reaches can be defined as losing water to GW, or gaining water from GW. Whether a stream reach is losing (GW recharge) or gaining (GW discharge) can be spatially and temporally dynamic, and can have substantial impacts on the hydrologic and solute characteristics of stream discharge.

[4] Stream water–GW exchange research at larger spatial and temporal scales has often relied on modeling mountain front GW recharge with limited data. Mountain front recharge (MFR) refers to the contributions from mountain regions to the GW recharge of adjacent basins [*Wilson and Guan*, 2004]. Efforts to understand and model MFR in arid to semiarid regions have increased as growing populations demand adequate and sustainable water supplies, particularly in the southwestern United States [*Phillips et al.*, 2004]. Significant GW withdrawals in the southwestern United States over the past several decades have led to GW depletion, land subsidence, decreased in-stream discharge, and loss of riparian habitat [*Phillips et al.*, 2004]. MFR has been noted as being a

[1] Land Resources and Environmental Sciences, Montana State University, Bozeman, Montana, USA.

0043-1397/07/2006WR005544$09.00

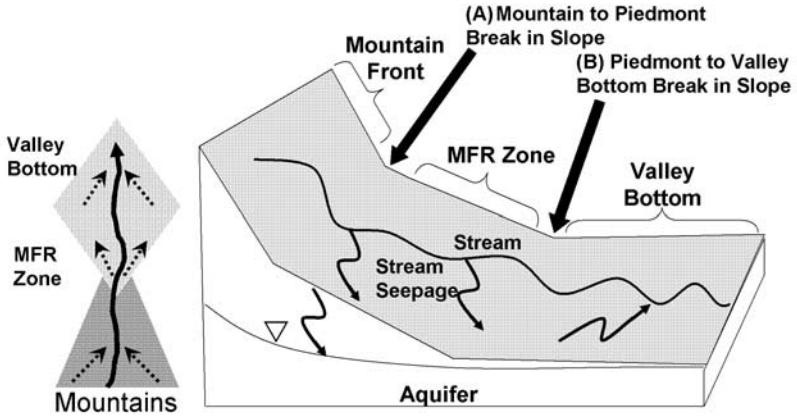

Figure 1. Conceptual diagram illustrating the mountain front recharge (MFR) zone, and the valley bottom in plan form and three-dimensional slice. The MFR zone is the region between points A and B. Arrows out of the stream represent stream seepage (groundwater recharge), and arrows into the stream represent groundwater discharge (adapted from *Wilson and Guan* [2004]).

major component of GW recharge in semiarid regions [*Manning and Solomon*, 2003]. MFR can occur either as percolation through the mountain block or as seepage losses from streams that exit the mountains. *Niswonger et al.* [2005] highlighted the importance of stream seepage MFR contributions to valley aquifers in the western United States. Although stream seepage MFR has been noted as being an important source of GW recharge to valley aquifers in arid to semiarid regions, it remains poorly understood and quantified [*Wilson and Guan*, 2004].

[5] Exchanges of water between streams and GW vary across different landscape elements (e.g., mountain front to valley bottom) within a watershed. Landscape elements that exist in a mountain watershed include mountain collection zone or mountain front, mountain front recharge (MFR) zone, and valley bottom zone. We define the mountain collection zone as the headwaters of the watershed where channels originate and are confined by topography, the MFR zone as the piedmont zone between points A and B on Figure 1 (modified from *Wilson and Guan* [2004]), and the valley bottom zone as the basin floor downstream of the MFR zone (Figure 1).

[6] Mountain collection zones typically have higher precipitation, lower evapotranspiration (ET), and less soil development than downslope landscape elements [*Wilson and Guan*, 2004]. Recent studies suggest that MFR is responsible for one third to nearly all of the GW recharge to intermountain basin fill aquifers [*Anderson and Freethey*, 1996; *Prudic and Herman*, 1996; *Mason*, 1998]. However, few studies have connected MFR to valley bottom hydrology. Investigating the hydrology and geochemistry of the stream and GW in both the MFR zone and the valley bottom zone allows determination of how stream water–GW exchanges can shift or vary from one landscape element to the next, and the impact these exchanges can have on watershed hydrologic response, discharge magnitude, source water mixing, and stream solutes.

[7] We used GW monitoring wells, in-stream piezometers, stream gauges, and geochemical hydrograph separation techniques in the Humphrey Creek watershed in southwestern Montana to address the following questions: (1) How do alpine to valley bottom transitions impact stream discharge?, and (2) how do stream gains and losses change across alpine to valley bottom transitions?

2. Study Area

[8] The Humphrey Creek watershed is located in the Centennial Mountains and Red Rock Lakes National Wildlife Refuge in southwestern Montana at 111.84°W longitude and 44.61°N latitude (Figure 2a). The continental divide forms the southern boundary of the watershed and Humphrey Creek flows from south to north. The Centennial Mountains are a block fault range and trend east–west. Humphrey Creek flows into Lower Red Rock Lake (LRRL) and drains a 351-ha watershed (Figure 2b). The Humphrey Creek watershed elevation ranges from 2012 to 2969 m. The headwaters of the creek begin above tree line in the alpine region of the watershed. Humphrey Creek then flows through subalpine mixed coniferous forest, exits the forest and flows through upland grasses, willows, and shrubs, and enters the valley bottom where the vegetation consists of sedges, rushes, grasses, and willows. The Humphrey Creek watershed is a mountain-to-valley transition watershed. These watersheds are commonly found in the American West and are critical to understanding water resources of the region.

[9] The area of instrumentation begins where Humphrey Creek exits the coniferous forest and continues to the lake edge (Figure 2c). Our instrumentation extends from the mountain front recharge (MFR) zone (where Humphrey Creek exits the coniferous forest) to the valley bottom zone (where Humphrey Creek enters LRRL).

[10] Average annual precipitation and snow water equivalent (SWE) data were obtained from the Lakeview Ridge Snowpack Telemetry (SNOTEL) site, which is located 1.5 km southeast of the Humphrey Creek watershed at an elevation of 2256 m. The 30-year average annual precipitation is 782 mm.

3. Methods

3.1. Groundwater Measurements

[11] We installed eight transects of wells (two to four wells per transect) perpendicular to Humphrey Creek from

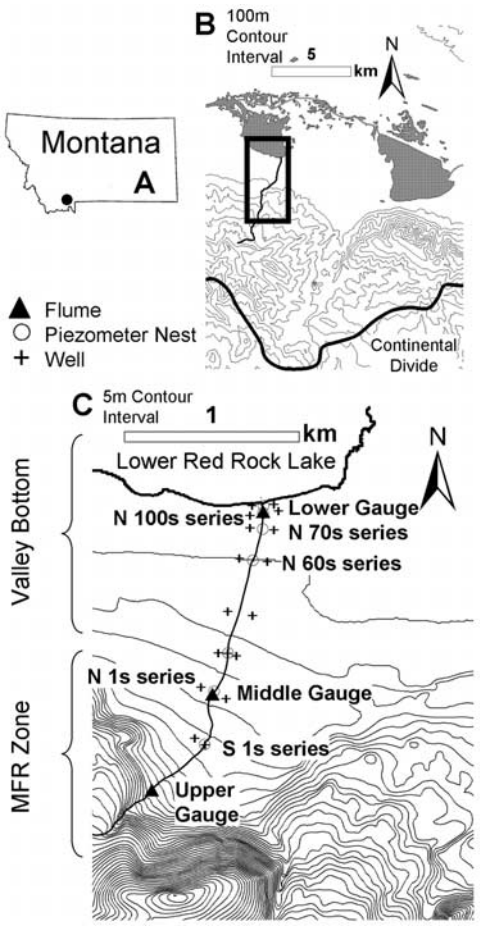

Figure 2. (a) Location of the Humphrey Creek watershed in southwestern Montana. (b) One-hundred-meter contour interval map showing the setting of the Humphrey Creek watershed in the Centennial Mountains, which form part of the continental divide. Lower Red Rock Lake elevation is 2015 m. (c) Five-meter contour map showing instrument layout (eight transects perpendicular to the stream channel), and delineation of the mountain front recharge (MFR) zone and the valley bottom zone in the Humphrey Creek watershed. Instrumentation includes seven piezometer nests (two piezometers per nest), 18 wells, and three stream gauging stations. N 100s series refers to the transect closest to the lake and includes north well 102 (NW102) and NW103. N 70s series refers to the third transect upstream of the lake and includes NW71/72 and north piezometer 70 (NP70) and NP71. N 60s series refers to the fourth transect upstream of the lake and includes NP61/62. N 1s series is the transect the middle gauge is on and includes NW1/4 and NP1/2. S 1s series is the transect between the middle and upper gauges and includes SW2/3 and SP1/2. Odd-numbered wells are on the west side of the stream, even-numbered are on the east, and piezometers are nested in the stream channel.

the upstream edge of the MFR zone to LRRL edge for GW sampling and to measure the dynamics of the local groundwater (GW) table adjacent to the stream (Figure 2c). Wells were 2-inch diameter, schedule 40, 0.01-inch screen, polyvinyl chloride (PVC). Well screening extended from well completion depths to approximately 10 cm below the ground surface. Most wells were instrumented with TruTrack, Inc., recording capacitance rods that recorded GW height (1-mm precision) and temperature (0.1°C precision) at 10-min intervals. We manually measured GW wells for depth to GW, GW specific conductance (SC), GW temperature, and GW solute concentrations at variable intervals depending on season (daily to weekly intervals). GW SC measurements were accurate to ±0.5% of the full scale of measurement.

[12] At the middle of each well transect we installed two nested piezometers in the streambed to determine the vertical GW gradients (Figure 2). Piezometers were 1.5-inch-diameter PVC pipe and were open only at completion depths (no screening). Piezometers were installed by driving them into the ground with a removable solid piezometer driver that occupied the volume of the PVC in order to keep them from filling with sediment. TruTrack, Inc., recording capacitance rods were installed in most piezometers and recorded GW height (total potential) and temperature at 10-min intervals. We manually measured GW total potential, SC, and temperature at variable intervals depending on season (daily to weekly intervals). Well and piezometer measurements began in March 2004 and continued through September 2004.

3.2. Stream, Soil, and Meteorological Measurements

[13] We installed three Parshall flumes (3-inch constriction) in Humphrey Creek during the spring of 2004: one in the upper reach of the study area, referred to as the upper gauge, a second in the middle reach of the study area, referred to as the middle gauge, and a third in the downstream reach of the study area, referred to as the lower gauge (Figure 2). The upper gauge was located at the upstream edge of the MFR zone near the point where the stream exited the mountain watershed, the middle gauge was located near the downstream edge of the MFR zone, and the lower gauge was located in the valley bottom zone near LRRL. We instrumented each flume with stage recording data loggers (either Druck pressure transducers and Campbell CR10X data loggers, or TruTrack, Inc., recording capacitance rods; 1-mm resolution) installed in stilling wells recording at 10-min intervals. Discharge was then calculated from developed stage-discharge rating curves. Stream gauging occurred over the full range of discharge at daily to weekly intervals (depending on season) either by salt dilution gauging or velocity area gauging with a Marsh-McBirney Flo-Mate Model 2000 portable flowmeter. Gauge measurements began at the end of April 2004 and continued until the end of September 2004.

[14] We recorded stream SC and stream temperature at the upper gauge, the middle gauge, and the lower gauge. Stream SC and temperature were measured with Campbell CS547A conductivity and temperature probes at 10-min intervals. Stream SC measurements were accurate to ±5% over a 0.44–7 mS cm^{-1} range, and ±10% over a 0.005–0.44 mS cm^{-1} range. We installed a Campbell TE525 tipping bucket rain gauge at the middle gauge to collect rain data, and a Thermocron I-button to record air temperature. The rain gauge recorded each 0.1 mm of rain, and air temperature was recorded at 10-min intervals with 1°C resolution.

3.3. Water Sampling and Solute Analysis

[15] GW samples were collected from wells, piezometers, and springs for chemical analysis. We used a handheld peristaltic pump and pumped and purged wells and lines before samples were collected. Stream samples were collected from gauging locations either as grab samples or with ISCO auto samplers. All samples were collected in 250-mL HDPE bottles and refrigerated at 4°C until filtering with 0.45-μm polypropylene filters and stored in the dark at 4°C until analysis.

[16] Water samples were analyzed for major ions with a Metrohm-Peak (Metrohm, Herisau, Switzerland) compact ion chromatograph at Montana State University. Sodium (Na), ammonium (NH_4), potassium (K), calcium (Ca), and magnesium (Mg) were measured on a Metrosep C-2-250 cation column. Nitrate (NO_3), chloride (Cl), phosphate (PO_4), and sulphate (SO_4) were measured on a Metrosep C-2-250 anion column. Standards and blanks were analyzed at the beginning of each sample run, were inserted between every 10 field water samples, and were analyzed at the back end of each sample run for quality assurance/quality control (QA/QC).

3.4. Hydrograph Separation and Uncertainty

[17] Hydrograph separations can be powerful tools for determining contributions to stream discharge from various sources (e.g., alpine zone surface water and valley bottom GW) [*McGlynn and McDonnell*, 2003]. If two sources contributing to stream discharge are unique, and their signatures are known, a two-component separation can be performed. We developed real-time separations for the middle gauge and the lower gauge using specific conductance (SC). Previous studies have used SC in hydrograph separations [*McDonnell et al.*, 1991; *Hasnain and Thayyen*, 1994; *Caissie et al.*, 1996; *Laudon and Slaymaker*, 1997; *Ahmad and Hasnain*, 2002; *Stewart et al.*, 2007]. *Laudon and Slaymaker* [1997] noted that the use of SC in hydrograph separations is appropriate in certain situations; however, use of SC should be verified against other, more conservative tracers. We corroborated the use of SC for hydrograph separations via comparison with separations based on calcium (Ca) and magnesium (Mg). Geochemical analysis of grab samples and regression of ion concentration versus SC revealed strong linear relationships between SC and Ca (R^2 = 0.949), and SC and Mg (R^2 = 0.932). Comparable results would have been obtained had hydrograph separations been based on either of these ion concentrations instead of basing separations on SC but would not have allowed real-time separations (10-min intervals). Snapshot-in-time separations were made using geochemical concentrations of groundwater and stream water samples, and were plotted against corresponding SC separations (R^2 = 0.977). The geochemical snapshot separations further validated hydrograph separations based on SC.

[18] We separated stream discharge into its alpine runoff (AL) and groundwater (GW) components. We defined AL as water exiting the mountains as channel flow at the upper gauge. Real-time (10-min interval) measurements of stream SC at the upper gauge were used to determine the signature of AL, and these values ranged from 0.074 to 0.305 mS cm^{-1}. The signature of GW was determined by averaging SC from ~100 groundwater samples. The average SC of these samples was 0.5 mS cm^{-1} and the standard deviation was ±0.188 mS cm^{-1}; this average and standard deviation were used as the GW end-member in hydrograph separations. This average value was obtained from samples of all wells and piezometers at daily to weekly intervals (dependent on season) over the duration of the study. SC at the middle gauge and the lower gauge was then a mixture of AL and GW components, and source water contributions could be separated real-time.

[19] A two-component separation can be solved by simultaneously solving equations (1), (2), and (3) [*Pinder and Jones*, 1969; *McGlynn et al.*, 2004]:

$$Q_{AL} = \left[\frac{C_{ST} - C_{GW}}{C_{AL} - C_{GW}}\right] Q_{ST} \tag{1}$$

$$Q_{GW} = \left[\frac{C_{ST} - C_{AL}}{C_{GW} - C_{AL}}\right] Q_{ST} \tag{2}$$

$$Q_{ST} = Q_{GW} + Q_{AL}, \tag{3}$$

where Q_{AL} is the contribution to discharge from alpine water, Q_{GW} is the contribution to discharge from valley bottom GW, Q_{ST} is stream discharge, C_{AL} is the tracer concentration (SC or a solute) of alpine water, C_{GW} is the tracer concentration of GW, and C_{ST} is the tracer concentration of stream water. We applied uncertainty analyses to the hydrograph separations following the methods of *Genereux* [1998] using equations (4) and (5).

$$W_{f_{AL}} = \left\{ \left[\frac{C_{GW} - C_{ST}}{(C_{GW} - C_{AL})^2} W_{C_{AL}}\right]^2 + \left[\frac{C_{ST} - C_{AL}}{(C_{GW} - C_{AL})^2} W_{C_{GW}}\right]^2 + \left[\frac{-1}{C_{GW} - C_{AL}} W_{C_{ST}}\right]^2 \right\}^{1/2} \tag{4}$$

$$W_{f_{GW}} = \left\{ \left[\frac{C_{AL} - C_{ST}}{(C_{AL} - C_{GW})^2} W_{C_{GW}}\right]^2 + \left[\frac{C_{ST} - C_{AL}}{(C_{AL} - C_{GW})^2} W_{C_{AL}}\right]^2 + \left[\frac{-1}{C_{AL} - C_{GW}} W_{C_{ST}}\right]^2 \right\}^{1/2} \tag{5}$$

where $W_{f_{AL}}$ is the uncertainty in the alpine component, $W_{f_{GW}}$ is the uncertainty in the GW component, $W_{C_{AL}}$ and $W_{C_{ST}}$ are the analytical errors in alpine and stream concentration measurements, $W_{C_{GW}}$ is the spatial variability in GW samples (standard deviation of GW samples), and C_{AL}, C_{GW}, and C_{ST} are alpine, GW, and stream concentrations (SC or a solute). In terms of analytical errors, the stream SC measurements were accurate to ±10% over a 0.005–0.44 mS cm^{-1} range and ±5% for values above 0.44 mS cm^{-1}, and GW SC measurements were accurate to ±0.5% of full scale of the measurement.

4. Results

4.1. Stream Discharge

[20] Stream discharge was greatest at the upper gauge where water exited the mountains and entered the mountain

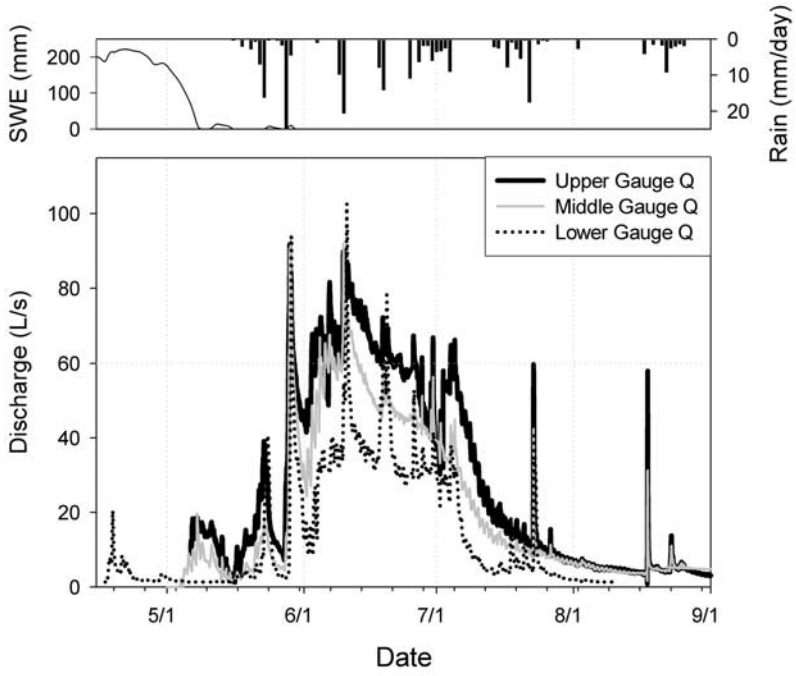

Figure 3. Stream hydrographs for the upper gauge located at the upstream edge of the mountain front recharge zone, the middle gauge located at the downstream edge of the mountain front recharge zone, and the lower gauge located in the valley bottom near the Lower Red Rock Lake edge.

front recharge (MFR) zone (Figure 3). The annual hydrograph at the upper gauge was driven primarily by mountain snowmelt and responded to rain events with rapid increases in discharge. Discharge was always greater at the upper gauge than the middle gauge, except for 28 May, when the middle gauge had a higher peak than the upper gauge. Although the middle gauge peak on 28 May was higher than the peak at the upper gauge, the total discharge for this day at the middle gauge amounted to only 73% of the total daily discharge at the upper gauge. The middle gauge annual discharge equaled ~77% of the upper gauge discharge (Table 1). The upper gauge and the middle gauge were located in the MFR zone, with the upper gauge at the upstream end of the MFR zone and the middle gauge near the downstream end of the MFR zone. We were unable to completely bracket the MFR zone and there were stream seepage losses that occurred downstream of the middle gauge. However, the discharge difference between the upper gauge and the middle gauge shows that ~23% of the water exiting the mountains as channel flow was lost from Humphrey Creek across this reach (Table 1).

[21] The hydrograph for the lower gauge, located in the valley bottom ~80 m upstream of Lower Red Rock Lake (LRRL), had a different hydrograph shape and duration than those for the upper gauge and the middle gauge (Figure 3). Discharge magnitude was less at the lower gauge compared with discharge in the MFR zone. Annual discharge at the lower gauge was 65% of the discharge at the middle gauge and 50% of the upper gauge discharge (Table 1).

4.2. Groundwater Well Hydrometric Data

[22] Depths to groundwater (GW) were typically greater than instrument completion depths in the mountain front recharge (MFR) zone. GW was not observed in south wells 2 (SW2) and 3 (SW3). These wells were located in the middle of the MFR zone (Figure 2c, part of the S 1s series). SW2 was completed to 1.64 m, and SW3 was completed to 0.98 m; rocky soils limited completion depths. The saturated zone began at some depth greater than 1.64 m on this transect. Further, GW levels in SW2 and SW3 were greater than the depth of the channel bed, resulting in a disconnected GW-stream system, i.e., no saturated connection between the stream and the GW table.

[23] Figure 4 displays north well 1 (NW1) and north well 4 (NW4) GW and local stream hydrograph time series. NW1 and NW4 were installed at the downstream end of the MFR zone (Figure 2c, part of the N 1s series). GW levels in these wells began to rise on 28 May. This rise in GW levels was coincident with a peak in local stream discharge and appears to have been initiated by a rain event on 28 May. Subsequently, GW levels in NW1 and NW4 rose and fell with the stream hydrograph. GW levels in NW4 receded more slowly than in NW1; however, because of the shallow completion of NW1 a complete analysis of the falling limb of GW levels in this well was not possible.

[24] Depths to GW in the valley bottom were shallow compared with GW depths in MFR zone. Figure 5 shows GW and local hydrograph time series for north wells 71 (NW71), NW72, NW102, and NW103 (see Figure 2c for well locations). A sharp rise in GW levels was measured in these wells on 20 March (Figure 5). After this initial rise, GW levels remained fairly constant over the course of the season. A small rise in GW levels in NW72 was measured between 28 May and 7 June, and peaked on 5 June (Figure 5). GW levels in the valley bottom zone were relatively unresponsive to rain events and were particularly unresponsive to local stream discharge. As GW levels in NW71 and NW72

Table 1. Total Discharge, Net Discharge, Gross Discharge Gains and Losses, and Percent Alpine (AL) and Groundwater (GW) Contributions for 2-Week Periods from 1 May to 15 August 2004[a]

Date Range	Upper Gauge Total Q, m^3	Middle Gauge Total Q, m^3	Lower Gauge Total Q, m^3	Net Δ Q Upper Middle, m^3	Gross Loss Upper Middle, m^3	Gross Gain Upper Middle, m^3	Net Δ Q Middle Lower, m^3	Gross Loss Middle Lower, m^3	Gross Gain Middle Lower, m^3	Middle Gauge, % AL	Middle Gauge, % GW	Lower Gauge, % AL	Lower Gauge, % GW
1–15 May	12,433	6,591	1,662	−5,842	−6,040	198	−4,929	−6,127	1,198	97	3	16	84
16–31 May	31,527	21,731	17,822	−9,796	−11,317	1,521	−3,909	−17,180	13,271	93	7	17	83
1–15 Jun	86,809	74,274	45,943	−12,535	−13,277	743	−28,331	−50,100	21,770	99	1	51	49
16–30 Jun	74,507	59,904	47,497	−14,603	−15,202	599	−12,407	−30,807	18,400	99	1	60	40
1–15 Jul	48,280	32,533	19,320	−15,747	−17,048	1,301	−13,214	−21,186	7,972	96	4	52	48
16–31 Jul	16,535	13,150	8,590	−3,385	−3,385	0	−4,560	−10,573	6,013	100	0	30	70
1–15 Aug	6,643	6,243	1,051	−400	−525	125	−5,192	−6,076	884	98	2	4	96
Total	276,735	214,427	141,886	−62,307	−66,794	4,487	−72,541	−142,050	69,509	97	3	33	67

[a]A negative net change in discharge represents a loss over the reach.

began to decrease in early August, channel flow at the lower gauge in the valley bottom decreased abruptly.

4.3. Piezometric Data

[25] Piezometer completion depths in the MFR zone were limited by rocky soils, and these vertically nested piezometers were typically dry, despite being located in the middle of the stream channel. Piezometers in the MFR zone included south piezometer 1 (SP1), south piezometer 2 (SP2), north piezometer 1 (NP1), and north piezometer 2 (NP2). SP1 and SP2 were located in the middle of the MFR zone, and NP1 and NP2 were located at the downstream end of the MFR zone (Figure 2c). Groundwater was not observed in SP1 or NP1 over the duration of the study. Total potential in NP2 began to rise on 28 May and subsequently rose and fell with the local stream hydrograph (Figure 6). Groundwater total potentials in the MFR zone were deeper than the channel bed, indicating hydraulic gradients out of the stream (stream water losses to groundwater). Humphrey Creek was a losing stream perched above the local GW table at our piezometer locations in the MFR zone. However, there may have been locations in the MFR zone where there was a saturated connection between the stream and the local GW.

[26] North piezometer 61 (NP 61) and north piezometer 62 (NP 62) were installed as a nest in the valley bottom zone (see Figure 2C for location). Total potentials in these piezometers were above the channel bed surface during periods of channel flow in the valley bottom, and upward vertical gradients were measured during this period (Figure 7). Groundwater total potentials in these piezometers peaked before local stream discharge, and strong upward groundwater gradients existed during peak discharge in the valley bottom zone. As groundwater total potentials in NP61 and NP62 fell below the channel bed surface during the middle of August, channel flow ceased in the valley bottom.

[27] Farther downstream toward LRRL, vertical groundwater gradients oscillated between upward, lateral (lateral flow), and downward (Figure 8). North piezometer 70 (NP70) and north piezometer 71 (NP71) were located in the valley bottom ~100 m upstream of the lower gauge (Figure 2c). Groundwater total potentials in NP70 and NP71 were consistently at or above the channel bed surface during times of channel flow in the valley bottom. As groundwater total potentials in NP70 and 71 dropped below the channel bed surface in mid-August, channel flow in the valley bottom ceased.

4.4. Stream Water Specific Conductance

[28] Stream water specific conductance (SC) was measured at the upper gauge, the middle gauge, and the lower gauge. SC at the upper gauge and the middle gauge was ~0.2 mS cm^{-1} during the rising limb and peak of the hydrographs for both of these gauges (Figure 9). The SC at the upper gauge and the middle gauge rose slightly during late season base flow (Figure 9). Rain events caused decreases in SC, due to increased contributions of low SC water to stream discharge. The lower gauge early season SC was much higher compared with the upper gauge and the middle gauge (Figure 9), and SC at the lower gauge was similar to groundwater SC (valley bottom groundwater conductivity was ~0.5 mS cm^{-1} ± 0.188 mS cm^{-1}). Stream

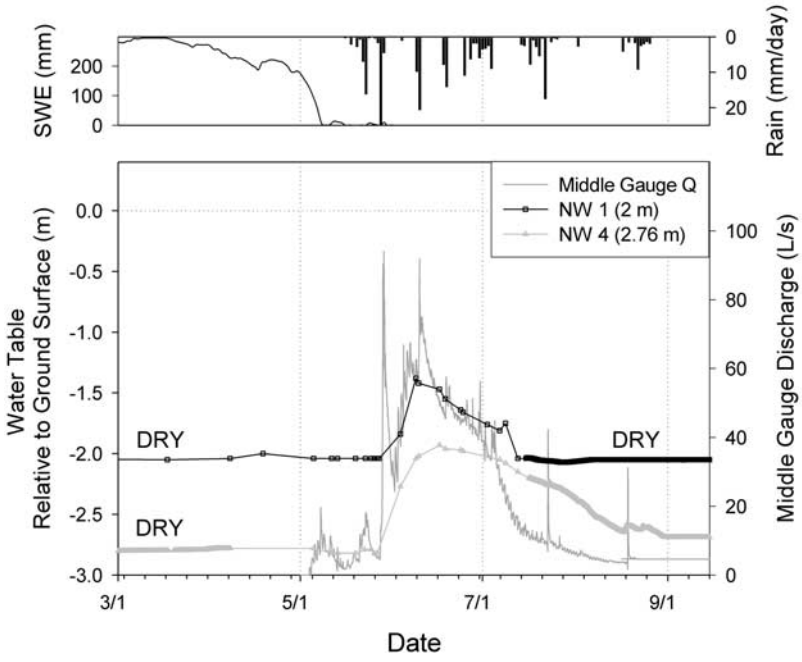

Figure 4. Water table dynamics for north well 1 (NW1) and NW4 (located at the down stream edge of the mountain front recharge zone).

SC at the lower gauge was ~0.6 mS cm^{-1} during early season (May), decreased to ~0.3 mS cm^{-1} during peak discharge (June), and rose to ~0.5 mS cm^{-1} during late season baseflow (July) (Figure 9).

4.5. Hydrograph Separations and Uncertainty Analysis

[29] Over the period of stream discharge at the middle gauge, groundwater contributions accounted for ~3% of total discharge, while alpine water comprised ~97% of total discharge (Figure 10a pie chart). Conversely, groundwater contributions over the period of stream discharge at the lower gauge were responsible for ~52% of the total discharge, while alpine water comprised ~48% of the total stream discharge (Figure 10b pie chart).

[30] Greatest groundwater contributions to stream discharge (~5% of total daily flow) were measured at the middle gauge during the rain induced hydrograph peak on 28 May (Figure 10a). From this time onward, including peak stream discharge, flow at the middle gauge was composed primarily of alpine water. In contrast, stream discharge at the lower gauge had substantial contributions from groundwater sources (Figure 10b). During early season flow (May), groundwater sources dominated stream discharge contributions at the lower gauge (~83% of total flow). Rain-induced peaks in discharge for the lower gauge were composed of ~93% groundwater during the 23 May peak, and ~78% groundwater during the 29 May peak. From 1 June to 5 July, groundwater contributions were responsible for ~50% of stream discharge at the lower gauge. From 5 July to 8 August, groundwater comprised ~71% of the water flowing in the channel at the lower gauge.

[31] Uncertainty is displayed as error bars on the hydrograph separation time series (Figure 10). Uncertainty was determined for each 10-min time step but was plotted once daily at noon on the hydrograph separation time series. Error bars show that uncertainty in the separations was not confounding and did not affect interpretation.

[32] Two-week discharge totals for the three gauges were determined and separated into groundwater and alpine water components for each 2-week period from the beginning of May through the middle of August (Figure 11c and Table 1). The total height of the bars in Figure 11c is equal to the total discharge for the 2-week period, the black portion of the bars is equal to the alpine contribution to discharge, and the gray portion of the bars is equal to the groundwater contribution to discharge. The upper gauge had the highest total discharge for all 2-week periods (Figure 11c and Table 1). The upper gauge discharge was composed completely of alpine water as the gauge was located at the mouth of the mountain watershed, and we defined stream water exiting the mountains as alpine water. The middle gauge discharge totals were less than the upper gauge discharge totals, and greater than the lower gauge discharge totals (Figure 11c and Table 1). Groundwater contributions to channel flow at the middle gauge were minor. The weeks from 16 May to 31 May had the greatest relative groundwater contributions to the middle gauge stream discharge, with groundwater accounting for ~7% of total flow (Table 1). The lower gauge stream discharge was composed of ~84% groundwater during weeks 1 May to 15 May and ~83% during weeks 16 May to 31 May (Figure 11 and Table 1). Alpine water contributions at the lower gauge were greatest during high flow between 1 June and 15 July, accounting for ~54% of total flow during this time period (Table 1). Groundwater comprised ~83% of late-season flow at the lower gauge between 16 July and 15 August (Table 1).

[33] We determined the net change between the upper and middle gauges, and the middle and lower gauges for each 2-week period (Figure 11b and Table 1). For all 2-week periods there were net losses between the upper and middle

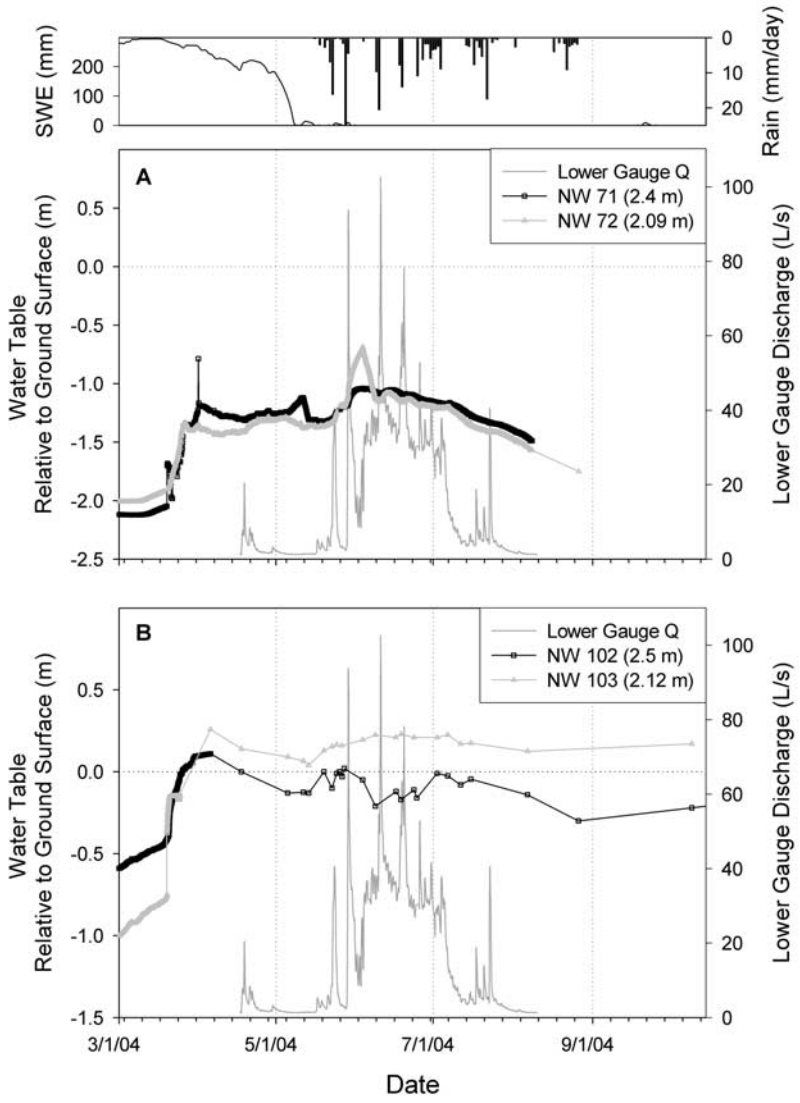

Figure 5. (a) Water table dynamics for north well 71 (NW71) and NW72 (located in the valley bottom) along with the local stream hydrograph; and (b) water table dynamics for north well 102 (NW102) and NW103 (located at the Lower Red Rock Lake Edge).

and the middle and lower gauges. Greatest net losses between the upper and middle gauges occurred during the 1 July to 15 July time period, and greatest losses between the middle and lower gauges occurred during the 1 June to 15 June time period (Table 1).

[34] We also determined the gross gains and losses between the upper and middle gauges, and the middle and lower gauges (Figure 11a and Table 1). Gross gains were equal to GW contributions to stream discharge between gauges, and gross losses were calculated as the difference between net change and gross gains. The gross losses between the upper and middle gauges were nearly equal to the net losses due to minimal gross gains. Conversely, gross gains between the middle and lower gauges were substantial but were less than gross losses leading to net losses between the two gauges (Figure 11a and Table 1).

[35] Variations in groundwater contributions to discharge peaks at the lower gauge can be seen in Figure 12. Discharge peaks on 5 May, 10 June, and 19 June are noted. It is apparent that groundwater contributions to stream discharge are greater during the rising than the falling limb of the annual hydrograph. During these peaks, groundwater accounts for ~78% of the 29 May (rising limb) total daily flow, ~47% of the total daily flow at peak discharge on 10 June, and ~34% of the 19 June peak (falling limb). There is also hysteresis in the annual discharge peak (10 June). Groundwater also accounts for more of the total discharge on the rising limb of the 10 June peak than on the falling limb (annotated on Figure 12 as "rising" and "falling").

5. Discussion

5.1. How Do Alpine to Valley Bottom Transitions Impact Stream Discharge?

[36] Stream discharge decreased moving downstream across the mountain front recharge (MFR) zone. Stream

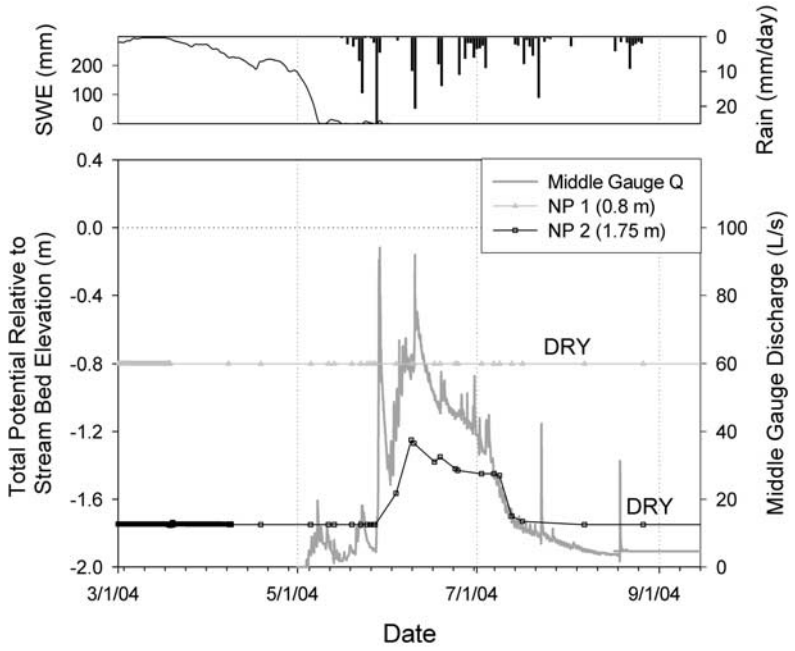

Figure 6. Groundwater dynamics for north piezometer 1 (NP1) and NP2 (located at the downstream edge of the MFR zone).

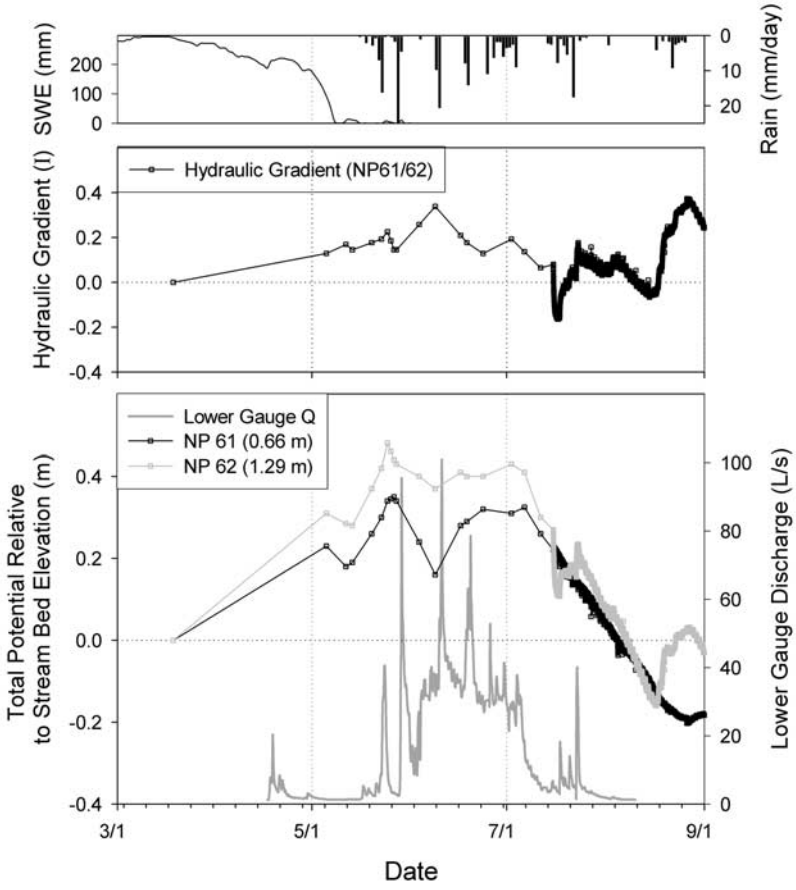

Figure 7. Groundwater dynamics for north piezometer 61 (NP61) and NP62 (located in the valley bottom).

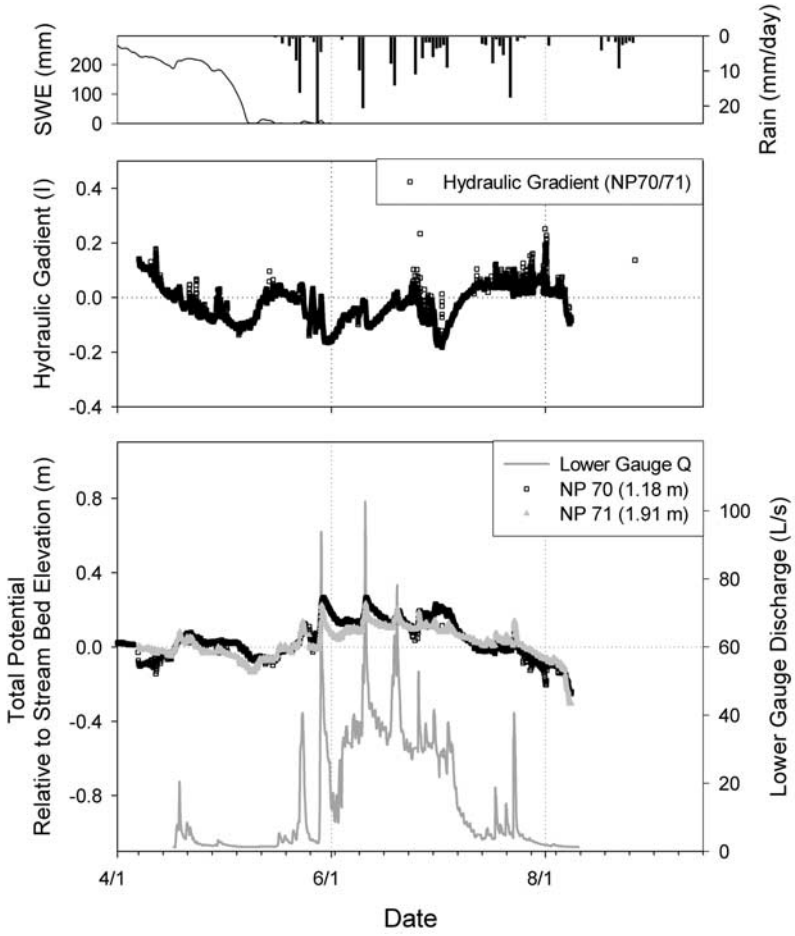

Figure 8. Groundwater dynamics for north piezometer 70 (NP70) and NP71 (located in the valley bottom).

losses in the MFR zone were partly driven by the physical disconnection between the stream and groundwater system (i.e., no continuous zone of saturation between the stream and groundwater). When a discontinuity between the stream and groundwater exists, stream seepage will occur and the rate of loss will be a function of stream stage, wetted perimeter, hydraulic conductivity, and bed armoring [*Niswonger et al.*, 2005].

[37] Stream seepage losses have been noted as an important source of groundwater recharge in the Basin and Range Province of the western United States, where streams exiting the mountains can lose the majority of their water as seepage [*Niswonger et al.*, 2005]. In the Humphrey Creek watershed, stream discharge at the lower gauge was 77% of the stream discharge at the upper gauge, which were both located in the MFR zone. Since there were minimal groundwater inputs to channel flow in this zone, a narrow riparian area (~0.7 ha), and no evidence of substantial stream water evaporation (that would have been evident by increased SC between the upper and middle gauges), we conclude that ~23% of stream water was lost as seepage across this reach. The stream gauges in the MFR zone were separated by ~0.5 km, and therefore ~23% of the stream water exiting the mountain watershed was lost from the stream in the first 0.5 km. If we assume constant seepage losses across the MFR zone (field observations indicate that stream water was not disproportionately lost in one location), ~126 m^3 of water per m of stream length (m^3 m^{-1}) would have been lost from the stream between 7 May and 23 August. This is equal to 1.2 m^3 m^{-1} d^{-1} of stream seepage losses contributing to groundwater and soil moisture recharge. The MFR zone stream gauging, groundwater levels, and hydrograph separation suggest that MFR zone stream seepage losses were an important source of groundwater recharge to the valley aquifer in the Humphrey Creek watershed and may be important in other basin aquifers adjacent to mountain watersheds.

[38] There was a net loss of stream water between the middle and lower gauges, but unlike the MFR zone there were substantial GW contributions to stream discharge in the valley bottom as well as losses from the stream. This net loss is because the net difference in discharge between two gauging locations is equal to the combination of the gross gains and gross losses over that reach. In a net loss situation the gross losses are larger than the gross gains, and the opposite is true in a net gaining reach. Over the 1 May to 15 August time period there was a gross loss of 142,050 m^3, a gross gain of 69,509 m^3, and a net loss of 72,541 m^3 between the middle and lower gauges. This illustrates the point that many streams do not simply lose or gain over a particular reach. It is more likely that many streams are both gaining and losing over the reach and that the net difference

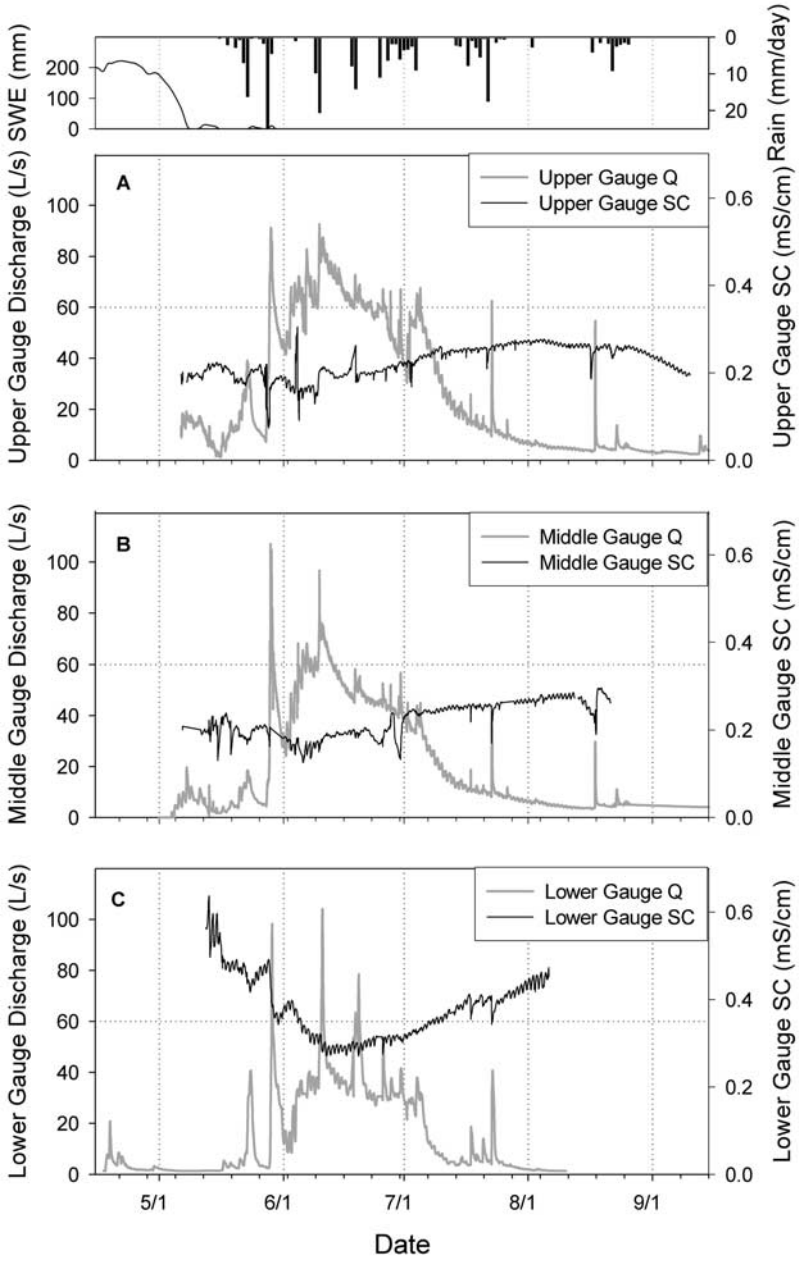

Figure 9. Stream hydrographs and stream specific conductance (SC) for (a) the upper gauge located at the upstream edge of the MFR zone; (b) the middle gauge located at the downstream edge of the MFR zone; and (c) the lower gauge located in the valley bottom near the Lower Red Rock Lake edge.

(if only discharge at two locations was measured) yields an incomplete assessment of the reach hydrology and gains/losses.

5.2. How Do Stream Gains and Losses Change Across Alpine to Valley Bottom Transitions?

[39] The area from the outlet of the mountain watershed to the beginning of the valley bottom was generally a groundwater recharge zone and was defined as the MFR zone. Since the GW inputs to stream discharge in the MFR zone were minimal, the stream water chemistry remained relatively constant between the upper gauge and the middle gauges. There were also stream losses that occurred downstream of the middle gauge. This highlights the difficulty in delineating the MFR zone with a single line. The edge of the MFR zone is a somewhat amorphous boundary that is difficult to capture with a stream gauge. It may be more appropriate to define the MFR zone hydrologically based on stream losses. The advantage of hydrograph separations in combination with discharge differences is the ability to determine gross gains and losses across the reach.

[40] There were GW inputs to the stream (GW discharge) in the valley bottom zone. As noted above, there were gross losses of 142,050 m^3 and gross gains of 69,509 m^3 across the valley bottom from 1 May to 15 August. Considering that *Harvey et al.* [1996] noted timescales of years for stream water–groundwater exchange on larger spatial scales, the water leaving the stream (gross losses) and the water entering the stream (gross gains) would not be expected to be the "same" water. This turnover of water

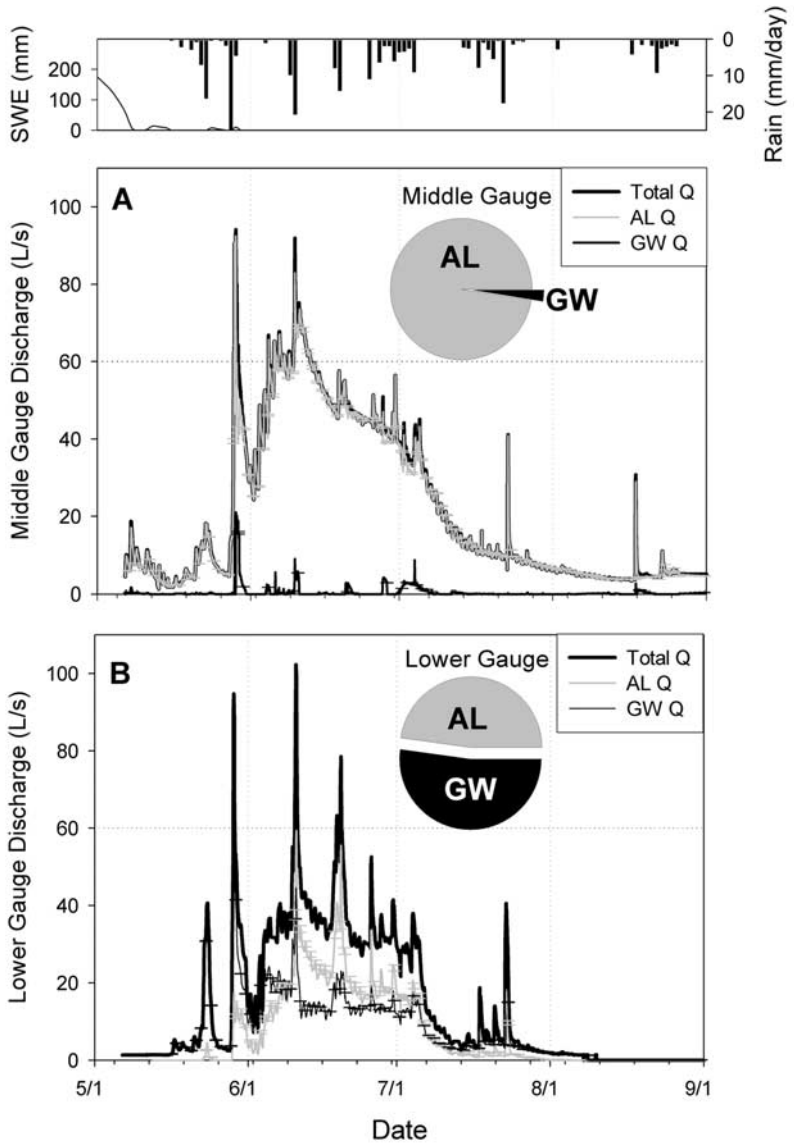

Figure 10. (A) Ten-minute-interval time series hydrograph separation for the middle gauge (located at the downstream edge of the MFR zone) into alpine runoff (AL) and groundwater (GW) contributions to stream discharge. Inset pie chart represents the alpine runoff and groundwater contributions to total discharge over 107 days. (b) Ten-minute-interval time series hydrograph separation for the lower gauge (located in the valley bottom at the upstream edge of Lower Red Rock Lake) into AL runoff and GW contributions to stream discharge. Inset pie chart represents the AL runoff and GW contributions to total discharge over 107 days.

flowing across the valley bottom has the effect of supplying "newer" water to the valley aquifer and "older" water back to the valley stream. This cycling of water from stream to valley aquifer back to stream has the ability to "reset" the stream water chemistry over short distances (~1 km for this study) as valley GW inputs begin to influence stream water chemistry. Also, GW inputs to valley stream discharge can have a large impact on the volume of channel flow in the valley: GW accounted for 52% of the total discharge at the lower gauge.

[41] These dynamic losses and gains observed here are important to note because it is likely that many mountain-to-valley transition streams function similarly. In these systems, water is moving into and out of the stream on spatial scales of kilometers and timescales of days to years and longer. Stream seepage across the MFR zone contributes to valley aquifer storage, and different stored valley GW contributes to valley stream discharge. These exchanges control stream discharge magnitude and solute characteristics, and valley aquifer storage state. Combining analysis of gross gains and losses with net differences in discharge is necessary to assess stream gains and losses over large spatial and temporal scales.

6. Conclusions

[42] Stream and groundwater hydrometric data coupled with geochemical hydrograph separations in the Humphrey

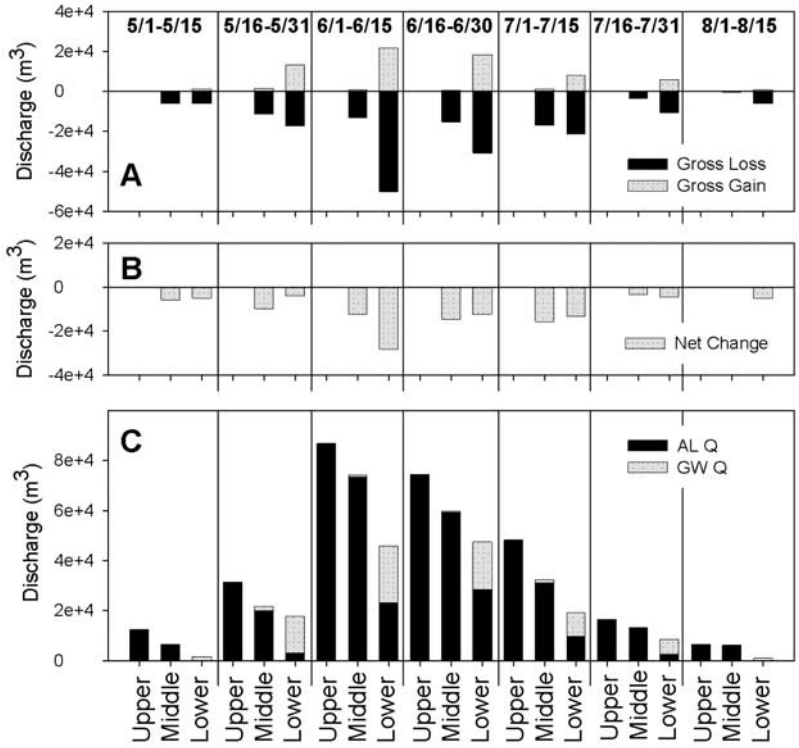

Figure 11. (a) Gross losses and gains over the upper to middle and middle to lower stream reaches for 2-week periods from 1 May to 15 August. Bars for the middle gauge refer to losses/gains over the upper to middle gauge reach. Bars for the lower gauge refer to losses/gains over the middle to lower gauge reach. (b) Net change in discharge over the reaches for each 2-week period. (c) Two-week total discharge separated into alpine runoff (AL) and groundwater (GW) contributions to stream discharge for the upper gauge, middle gauge, and lower gauge. The upper gauge was located at the upstream edge of the mountain front recharge (MFR) zone, and upper gauge stream discharge was defined as alpine runoff. The middle gauge was located at the downstream edge of the MFR zone, and the lower gauge was located in the valley bottom near the Lower Red Rock Lake edge.

Creek watershed of southwestern Montana suggest that (1) stream seepage losses are an important source of recharge to valley aquifers adjacent to mountain watersheds, (2) valley bottom groundwater contributions are important to valley stream discharge, and can help sustain channel flow, (3) dynamic stream gains and losses are important to valley aquifer status and can set valley stream water chemistry, and (4) it is important to realize that net differences in discharge are the sum of the gross gains and losses across the reach and it is likely that many streams are losing in some locations while gaining in others.

[43] This research suggests a conceptual model where mountain runoff contributes to valley aquifer recharge and different stored water in the valley aquifer contributes back to valley stream discharge. Mountain collection zones collect precipitation and focus stream discharge, as this stream discharge moves toward the adjacent alluvial valley much of it is lost as stream seepage in the MFR zone. Stream seepage then contributes to valley aquifer storage. In turn, water previously stored in the valley aquifer discharges to the valley stream impacting valley stream discharge and chemistry. This cycling of water, and not the one-to-one replacement often implied by exchange, is important to recognize because it has implications for stream water chemistry and for estimates of GW storage and movement.

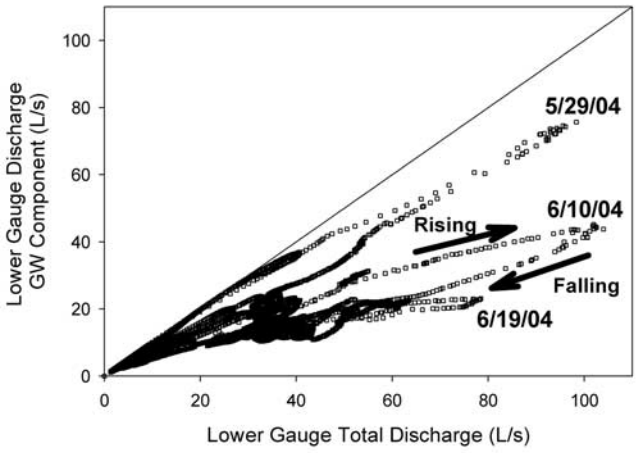

Figure 12. Bivariate plot of GW contributions to lower gauge stream discharge versus total discharge at the lower gauge. Three peaks in discharge noted: 29 May, 10 June, and 19 June. Rising and falling refer to hysteresis in 10 June hydrograph peak.

[44] As water is lost from the stream and stored water enters the stream in the valley bottom, the stream chemistry changes due to the influence of the valley aquifer inputs. These inputs also affect the amount of water flowing across the valley floor. GW contributions to stream discharge are likely to be from stored water close to the stream channel, and as such GW contributions to stream discharge in response to MFR may be quite rapid. However, MFR contributing to the valley aquifer may be stored for years before reentering the valley stream. Stream water–GW research should be conscious of the dynamic stream gains and losses over timescales of hours to years and spatial scales of kilometers.

[45] The results presented here warrant further investigation into stream gains and losses across the spatial and temporal scales we have investigated. Since the mountain to alluvial aquifer transition is a dominant landscape of the American West and crucial to water resources in this region, it is imperative that future research develop a further understanding of stream gains/losses across the mountain-to-valley transition and how these affect valley aquifers and streams.

[46] **Acknowledgments.** The authors thank Stephen Custer, William Inskeep, and Richard Sojda for comments that improved the quality of this work, and Brian Edwards for help collecting field data. We would also like to thank the Red Rock Lakes Wildlife Refuge for support and access to field sites. This project was partially funded by the Montana Water Center USGS 104b program and National Science Foundation grant EAR-0337650.

References

Ahmad, S., and S. I. Hasnain (2002), Hydrograph separation by measurement of electrical conductivity and discharge for meltwaters in the Ganga headwater basin, Garhwal Himalaya, *J. Geol. Soc. India*, *59*, 323–329.

Anderson, T. W., and G. W. Freethey (1996), Simulation of ground-water flow in alluvial basins in south-central Arizona and adjacent states, *U.S. Geol. Surv. Prof. Pap.*, *1406-D*, 78 pp.

Caissie, D., T. L. Pollock, and R. A. Cunjak (1996), Variation in stream water chemistry and hydrograph separation in a small drainage basin, *J. Hydrol.*, *178*, 137–157.

Genereux, D. (1998), Quantifying uncertainty in tracer-based hydrograph separations, *Water Resour. Res.*, *34*, 915–919.

Harvey, J. W., B. J. Wagner, and K. E. Bencala (1996), Evaluating the reliability of the stream tracer approach to characterize stream-subsurface water exchange, *Water Resour. Res.*, *32*, 2441–2451.

Hasnain, S. I., and R. J. Thayyen (1994), Hydrograph separation of bulk meltwaters of Dokriani-Bamak Glacier Basin, based on electrical-conductivity, *Curr. Sci.*, *67*, 189–193.

Laudon, H., and O. Slaymaker (1997), Hydrograph separation using stable isotopes, silica and electrical conductivity: An alpine example, *J. Hydrol.*, *201*, 82–102.

Malard, F., K. Tockner, M. J. Dole-Olivier, and J. V. Ward (2002), A landscape perspective of surface-subsurface hydrological exchanges in river corridors, *Freshwater Biol.*, *47*, 621–640.

Manning, A. H., and D. K. Solomon (2003), Using noble gases to investigate mountain-front recharge, *J. Hydrol.*, *275*, 194–207.

Mason, J. L. (1998), Ground-water hydrology and simulated effects of development in the Milford area, an arid basin in south-western Utah, *U.S. Geol. Surv. Prof. Pap.*, *1409-G*, 69 pp.

McDonnell, J. J., M. K. Stewart, and I. F. Owens (1991), Effect of catchment-scale subsurface mixing on stream isotopic response, *Water Resour. Res.*, *27*, 3065–3073.

McGlynn, B. L., and J. J. McDonnell (2003), Quantifying the relative contributions of riparian and hillslope zones to catchment runoff, *Water Resour. Res.*, *39*(11), 1310, doi:10.1029/2003WR002091.

McGlynn, B. L., J. J. McDonnell, J. Seibert, and C. Kendall (2004), Scale effects on headwater catchment runoff timing, flow sources, and groundwater-streamflow relations, *Water Resour. Res.*, *40*, W07504, doi:10.1029/2003WR002494.

Niswonger, R. G., D. E. Prudic, G. Pohll, and J. Constantz (2005), Incorporating seepage losses into the unsteady streamflow equations for simulating intermittent flow along mountain front streams, *Water Resour. Res.*, *41*, W06006, doi:10.1029/2004WR003677.

Oxtobee, J. P. A., and K. Novakowski (2002), A field investigation of groundwater/surface water interaction in a fractured bedrock environment, *J. Hydrol.*, *269*, 169–193.

Phillips, F. M., J. F. Hogan, and B. R. Scanlon (2004), Introduction and overview, in *Groundwater Recharge in a Desert Environment: The Southwestern United States*, *Water Sci. Appl. Ser.*, vol. 9, edited by J. F. Hogan et al., pp. 1–14, AGU, Washington, D. C.

Pinder, G. F., and J. F. Jones (1969), Determination of the groundwater component of peak discharge from the chemistry of total runoff, *Water Resour. Res.*, *5*, 438–445.

Prudic, D. E., and M. E. Herman (1996), Ground-water flow and simulated effects of development in Paradise Valley, a basin tributary to the Humboldt River in Humboldt County, Nevada, *U.S. Geol. Surv. Prof. Pap.*, *1409-F*, 92 pp.

Ren, J. H., and A. I. Packman (2005), Coupled stream-subsurface exchange of colloidal hematite and dissolved zinc, copper, and phosphate, *Environ. Sci. Technol.*, *39*, 6387–6394.

Stewart, M., J. Cimino, and M. Ross (2007), Calibration of base flow separation methods with streamflow conductivity, *Ground Water*, *45*, 17–27.

Wagner, F. H., and C. Beisser (2005), Does carbon enrichment affect hyporheic invertebrates in a gravel stream?, *Hydrobiologia*, *544*, 189–200.

Wilson, J. L., and H. Guan (2004), Mountain-block hydrology and mountain front recharge, in *Groundwater Recharge in a Desert Environment: The Southwestern United States*, *Water Sci. Appl. Ser.*, vol. 9, edited by J. F. Hogan et al., pp. 113–137, AGU, Washington, D. C.

Wroblicky, G. J., M. E. Campana, H. M. Valett, and C. N. Dahm (1998), Seasonal variation in surface-subsurface water exchange and lateral hyporheic area of two stream-aquifer systems, *Water Resour. Res.*, *34*, 317–328.

T. P. Covino and B. L. McGlynn, Land Resources and Environmental Sciences, Montana State University, 334 Leon Johnson Hall, Bozeman, MT 59717, USA. (timothy.covino@myportal.montana.edu)